Bull. Fish. Sci. Hokkaido Univ.
55(2), 105-119, 2004.

Winter Transport and Tidal Current in the Tsugaru Strait

Mitsuyo ONISHI[1)], Yutaka ISODA[1)], Hiroshi KURODA[1)],
Masayuki IWAHASHI[1)], Chizuru SATOH[1)], Tomoharu NAKAYAMA[2)],
Toshimichi ITO[3)], Kenichi ISEDA[2)], Keisuke NISHIZAWA[2)],
Shigeki SHIMA[2)] and Orihiko TOGAWA[3)]

(Received 26 March 2004, Accepted 9 August 2004)

Abstract

Transport variations and characteristics of tidal currents in the Tsugaru Strait are investigated using the ship-mounted acoustic Doppler current profiler (ADCP) measurements from October 29, 1999 to March 31, 2000 along one line across the Strait. The Tsugaru Strait connects the North Pacific Ocean and Japan/East Sea, and is a main output for Tsushima Warm Current System in Japan/East Sea. The strong northeastwards mean current flows through this section approximately in the center of the Strait, and southwestward counter flows exist near both the Hokkaido and Honshu coasts. The estimated mean net eastward transport, i.e., the Tsugaru Warm Current transport, is 1.8 Sv (Sverdrup, 1 Sv = 10^6 m^3s^{-1}). The data are analyzed four major tidal constituents, i.e., M2, S2, O1 and K1. Although the amplitudes of semi-diurnal tides are generally larger than those of diurnal tides, the amplitudes of K1 and M2 volume transports across the strait are 0.72 Sv and 0.52 Sv, respectively, i.e., diurnal tidal currents are dominant. From the phase relationship between tidal volume transport and tide is understood with a composite of standing and incident Kelvin waves, which propagates from the North Pacific Ocean to the Japan/East Sea. We also find a significant fortnightly oscillation which has a barotropic structure. The long-period lunar fortnightly (Mf) tide is more energetic along the coast faced on the Japan/East Sea with the amplitude of 1 ~3 cm, while the amplitudes for Mf tide in the North Pacific Ocean are much smaller, less than 1 cm. It is inferred that observed fortnightly oscillation may be generated by the difference of Mf tide amplitude between both sides of the Tsugaru Strait.

Key words: Tsugaru Strait, ADCP, Volume transport, tidal current

Introduction

Figure 1(a) illustrates the typical current systems around the Japanese islands, and Figure 1(b) shows the bathymetry in the Tsugaru Strait (hereafter, referred to as "the Strait"). The Strait is a narrow and shallow connecting channel between the North Pacific Ocean that is broad and deep (depth is not less than 4,000 m) and the Japan/East Sea (mean depth is about 1,350 m). In general, the dimensions of the Strait are about 100 km in length and 20~40 km in width, and a mean water depth of it is about 150 m. Currents in the Strait are characterized by the coexistence of the strong tidal currents and the eastward flow of the Tsugaru Warm Current (TWC). TWC is a branching flow of the Tsushima Warm Current that transfers heat, salt, fish larvae from the Japan/East Sea to the Oyashio Region in the North Pacific Ocean. The Strait is also known as one of the important international shipping lane routes in Asia, and as a good fishing ground of cuttlefish (*Todarodes pacificus*).

Long-term measurements of currents in the Strait are rare because of the strong fishing activities and much traffic density of ships. Recently, Shikama (1994) found that the annual mean volume transport of TWC was about 1.4 Sv using bottom fixed acoustic Doppler current profilers (ADCPs). As long as we know, this was the only long-term measurement of the Strait, but he did not discuss the characteristics of tidal currents. On the other hand, there were many studies in which

[1,2)] *Mutsu Marine Laboratory, Japan Marine Science Foundation*
(日本海洋科学財団むつ海洋研究所)
[3)] *Marine Research Laboratory, Japan Atomic Energy Research Institute*
(日本原子力研究所)
[1)] Present address: Graduate School of Fisheries Sciences, Hokkaido University
(e-mail: hatter@sola3.fish.hokudai.ac.jp (M. Onishi))
(北海道大学大学院水産科学研究科)

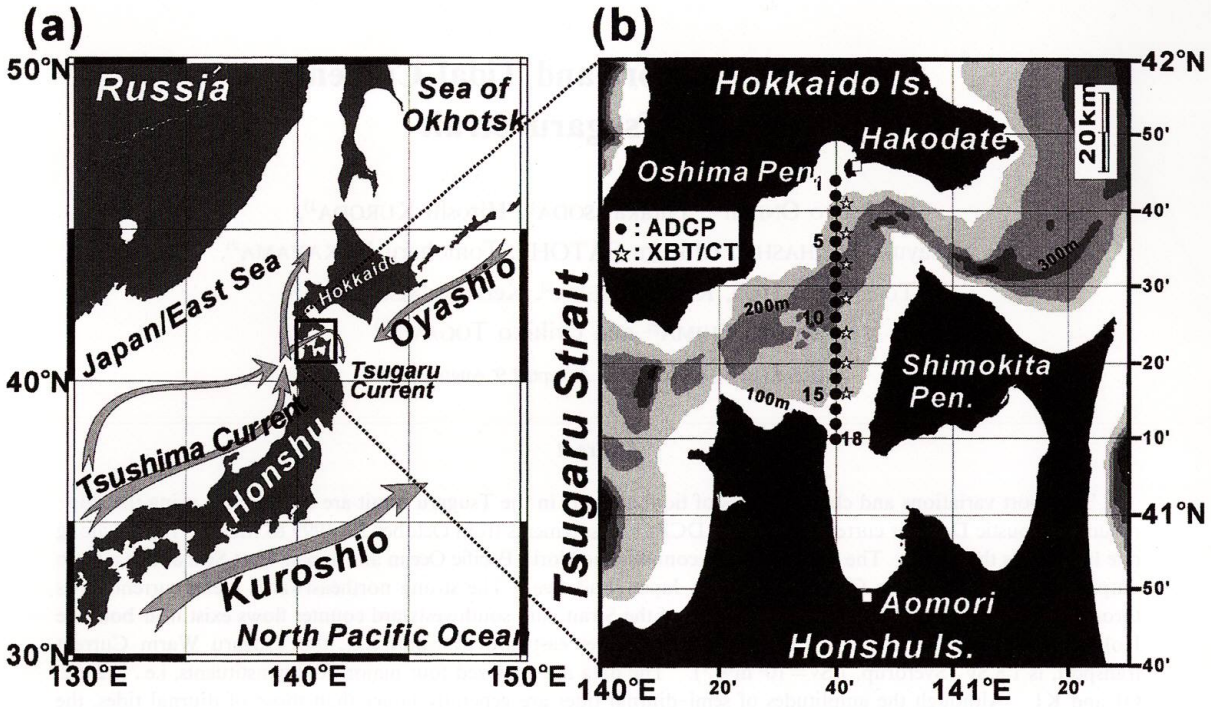

Fig. 1. Map of the Japan and the adjacent seas with schematic representation of current systems, study area (a). Also shown are the location of chosen delegate 18 stations of ADCP data (solid circles) and locations of observation points of XBT and CTD (star) (b).

short-term current measurements were conducted and coastal tide data were obtained (Ogura (1932, 1933), Hikosaka (1953), Nitani et al. (1959), Kubota and Iwasa (1961), Hori and Nitta (1978) and Odamaki (1984)). The conception of tides in the Strait employed in the present study was provided by Ogura (1932). Ogura (1932) first edited the co-tidal and co-range charts of tide using the tidal harmonic constants at the coastal tidal stations. As examples of semi-diurnal and diurnal tides, the amplitude and phase charts of K1 and M2 tides are shown in Figures 2(a) and (b). He described the tides in the Strait as the oscillations in a longitudinal direction along the axis of the Strait that was formed due to the mixture of the tide waves incoming from the Japan/East Sea and the North Pacific Ocean. Recently, Odamaki (1984) estimated the general strengths of the tide and tidal currents, by reanalyzing a half-month current measurement data (Japan Coast Guard). He showed that the diurnal tidal current speed was larger than the semi-diurnal one near the eastern and western entrances of the Strait, while the semi-diurnal tide was larger than the diurnal one along the whole coastal tidal stations. He also suggested that the semi-diurnal tides were standing waves, and the diurnal tides were composed of standing and progressive waves. However, both the tidal current phases and speeds are marked by strong spatial variability across the Strait, as discussed later in this paper.

The recent development of ship-mounted ADCPs enables us to perform long-term measurements of the Strait. It is possible to determine the cross-strait and vertical current structures of tides and mean flows using our ship-mounted ADCP measurements. This study analyses the data obtained at 18 points across the Strait in winter, which are located on the north-south line spanning the central part of the Strait (see Figure 1(b)). The purpose of this measurement is to delineate the structure of the currents and tides, and thus to gain a better understanding of their dynamics and the estimation of winter season transport in the Strait.

Observations and Data Process

The ship-mounted ADCP measurements are carried out across the Strait during 5 months between October, 29 1999 and March, 31 2000 by using a regular shuttling ferryboat M.V. *Virgo* (134.6 m, 6,358 t, HIGASHI-NIHON-FERRY Co., Ltd.), which plies between Aomori and Hakodate 2 times a day. Table 1 shows periods of acquisition of the data. ADCP installed in M.V. *Virgo* is a RD Instrument ADCP operating 150 kHz. The transducer is set 5 m below the sea surface, and the first depth bin is 17 m below the surface. Since the deepest depth of the transect is about 220 m, all the ADCP data can refer to the sea bottom. The ADCP internal processing type is selected to be Mode-1 (the

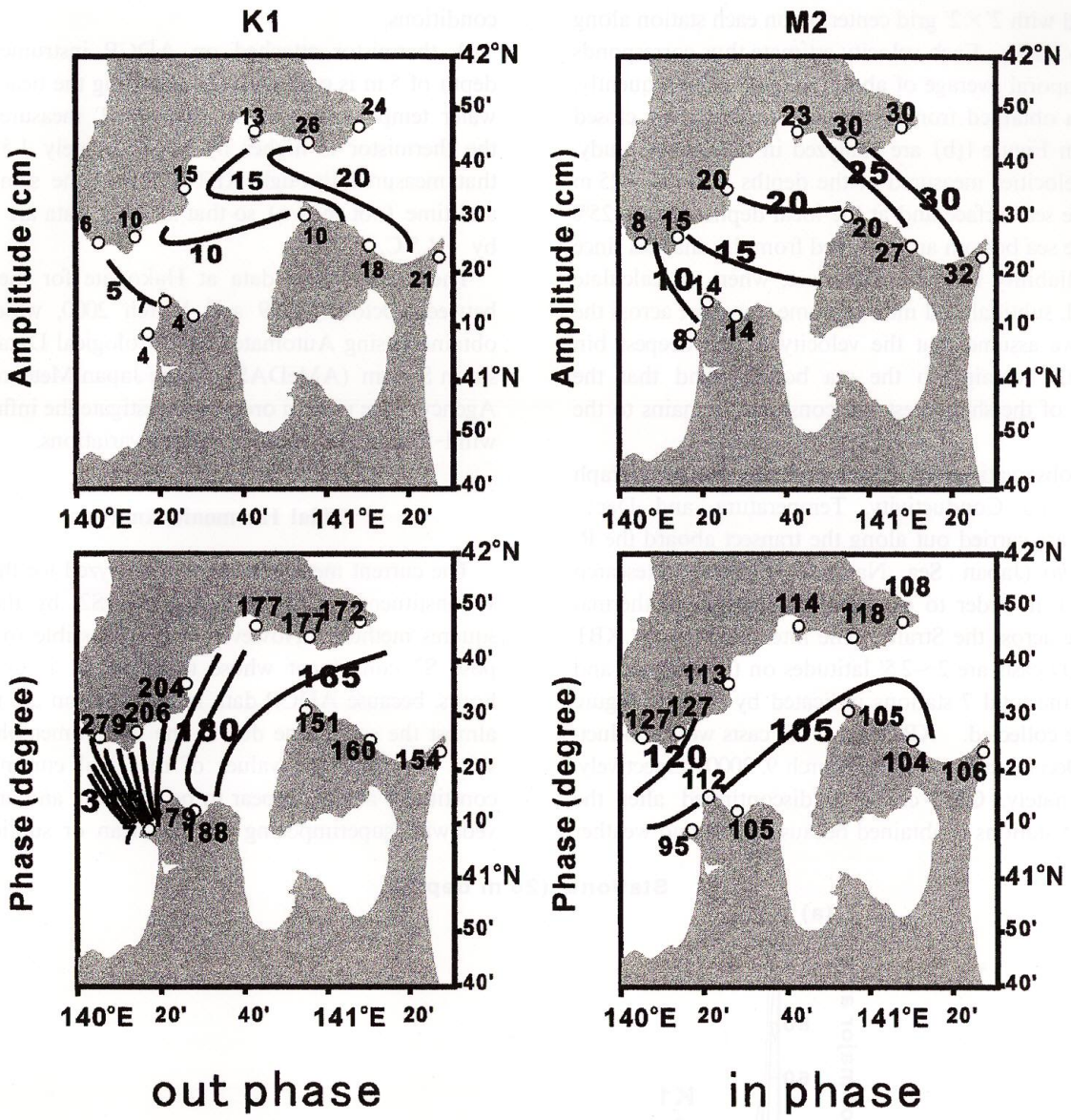

Fig. 2. The co-tidal charts for K1 and M2 tide. Deduced from analysis of 12 tide point (solid circle). Amplitude line (upper panels) are in centimeters and contour interval is 5 cm. Phase lines are in degrees with respect to Japan Standard Longitude (JSL : 135° E) and contour interval is 15°.

Table 1. Periods of acquisition of *VIRGO* ADCP data

No.	Start time		Stop time
1	99/10/29 18 : 02	—	99/11/10 07 : 32
2	99/11/12 12 : 07	—	99/11/24 02 : 03
3	99/11/26 12 : 17	—	99/12/08 02 : 22
4	99/12/10 12 : 01	—	99/12/21 23 : 01
5	99/12/24 12 : 02	—	00/01/04 23 : 54
6	00/01/07 11 : 58	—	00/01/19 02 : 19
7	00/01/21 12 : 00	—	00/02/02 05 : 40
8	00/02/04 11 : 59	—	00/02/14 14 : 47
9	00/02/18 08 : 43	—	00/03/01 00 : 11
10	00/03/03 11 : 56	—	00/03/15 03 : 15
11	00/03/17 12 : 05	—	00/03/29 06 : 42

condition for heavy shear and rigorous vessel motion). The nominal vertical resolution is 4 m, and the profiles of velocity components are recorded at 80 sec intervals. Although the first depth bin for obtaining ACDP data is set to be 17 m from the sea surface at first, only the data at the depths of more than 25 m are effective since signals obtained near the bottom of the ship are insufficient. We exclude the ADCP data within 25% of the local depth originating from the sea bottom, because of the acoustic side lobe interference. We then remove spurious data which meet with the following exclusion criteria: data with the percent good pings of less than 90%. For the discrete station with the horizontal interval within latitude 2′, we average the ADCP data

acquired with 2′×2′ grid centering on each station along the ship track. Each velocity estimate thus corresponds to a temporal average of about 10 min. Consequently, the data obtained from 18 stations indicated by closed circles in Figure 1(b) are analyzed in the present study. Since velocities measured at the depths of 0 to −25 m from the sea surface and at the local depths of 0 to 25% from the sea bottom are excluded from the analysis since their reliability is low. Therefore, when we calculate the tidal, subtidal and mean volume transport across the Strait, we assume that the velocity of the deepest bin constantly remains to the sea bottom, and that the velocity of the shallowest bin constantly remains to the surface.

The observations of Expendable Bathythermograph (XBT), and Conductivity, Temperature, and Depth (CTD) are carried out along the transect aboard the R. V. *Mizuho* (Japan Sea National Fisheries Research Institute), in order to examine the changes of thermal structure across the Strait. The intervals between XBT and CTD casts are 2~2.5′ latitudes on the transect, and data at the total 7 stations indicated by stars in Figure 1(b) are collected. XBT and CTD casts were conducted on December 7, 1999 and March 9, 2000, respectively. Unfortunately, CTD-cruise is discontinued after the data of 5 stations is obtained because of the bad weather conditions.

A thermistor attached on ADCP instrument at a depth of 5 m is continuously recording the near-surface water temperature (NST). The NST measured using the thermistor is higher by approximately 1.5°C than that measured through XBT/CTD at the same depth and time (not shown), so that all NST data are rectified by −1.5°C.

The hourly wind data at Hakodate for the period between October 1999 and March 2000, which were obtained using Automated Meteorological Data Acquisition System (AMeDAS) by the Japan Meteorological Agency, were used in order to investigate the influence of wind-forcing on subtidal current variations.

Tidal Harmonic Analysis

The current measurements are analyzed for the major 4 constituents of O1, K1, M2 and S2, by the least-squares method. However, it is impossible to decompose S2 constituent whose tidal period is exactly 12 hours, because ADCP data in each station are taken at almost the same time due to the fixed timetable of the ship. Namely, the values of the tidal current of S2 constituent always appear to be constant, and are observed with superimposing on the mean or subtidal cur-

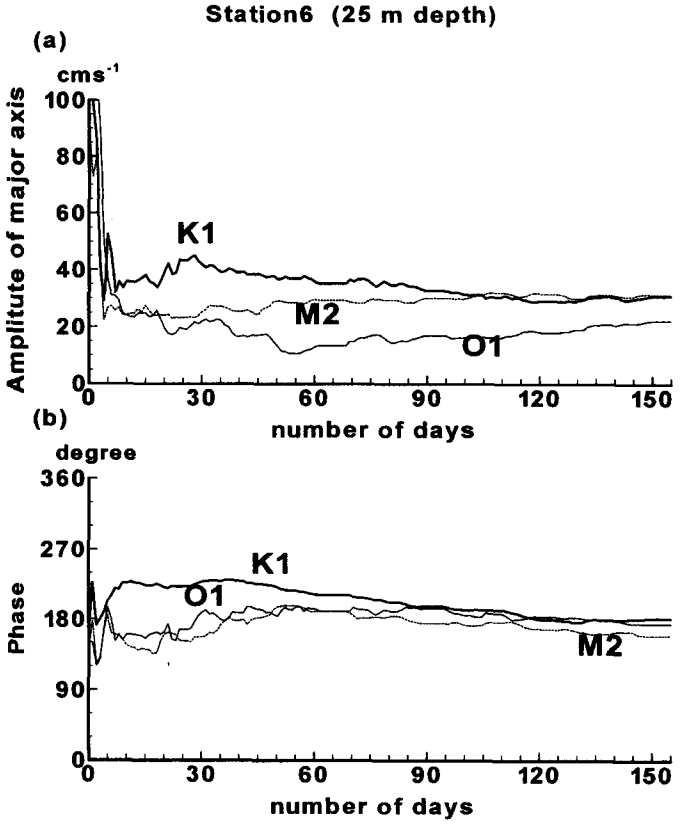

Fig. 3. The dependence of obtained harmonic constants on the number of days, amplitudes (a) and Phases (b). Thick line is K1 constituent, thin line is O1 constituent and dashed line is M2 constituent.

rents. Therefore, we must decompose S2 constituent and remove it from the original data. Odamaki (1989) proposed the method for removing undecomposed harmonic constant of the tidal species, when the relations of the amplitude ratio and phase differences between two tidal constituents were known. Of course, it is assumed that the tidal constituents whose periods are close to each other indicate similar dynamics of tide. According to his method, the following equations for S2 harmonic constants, using an amplitude ratio (γ) and a phase difference ($\Delta\kappa$), between S2 and M2 tidal currents are assumed:

$$H_{S2}=\gamma H_{M2}$$
$$\kappa_{S2}=\Delta\kappa+\kappa_{M2}$$

where H and κ are the amplitude and phase of each constituent, respectively. In the Strait, γ is 0.46, and $\Delta\kappa$ is 38°, which are mean values of the harmonic constants estimated using a half-month observation data at the eastern and western entrances in the Strait (Odamaki, 1984). Based on the above relations, the harmonic constants of S2 constituent can be included in those of M2 constituent.

Next, we check the necessary number of ADCP data to obtain the stable harmonic constants. The dependence of obtained harmonic constants on the used data period (the number of days) at 25 m depth of Station (Stn.) 6, where the tidal current dominates the most among all the stations, is shown in Figure 3. Although the increasing number of days causes the long-term trend which arises from distortion for excluding the other minor tidal constituents such as P1, N2 and K2, it is found that about 100 days are necessary to obtain the stable harmonic constants of M2 and K1 constituents, and about 150 days to O1 constituent. In the present harmonic analysis, therefore, we use all data obtained for the period of 155 days.

Results

Thermal structures across the Strait in winter

Figures 4(a) and (b) show the vertical distributions

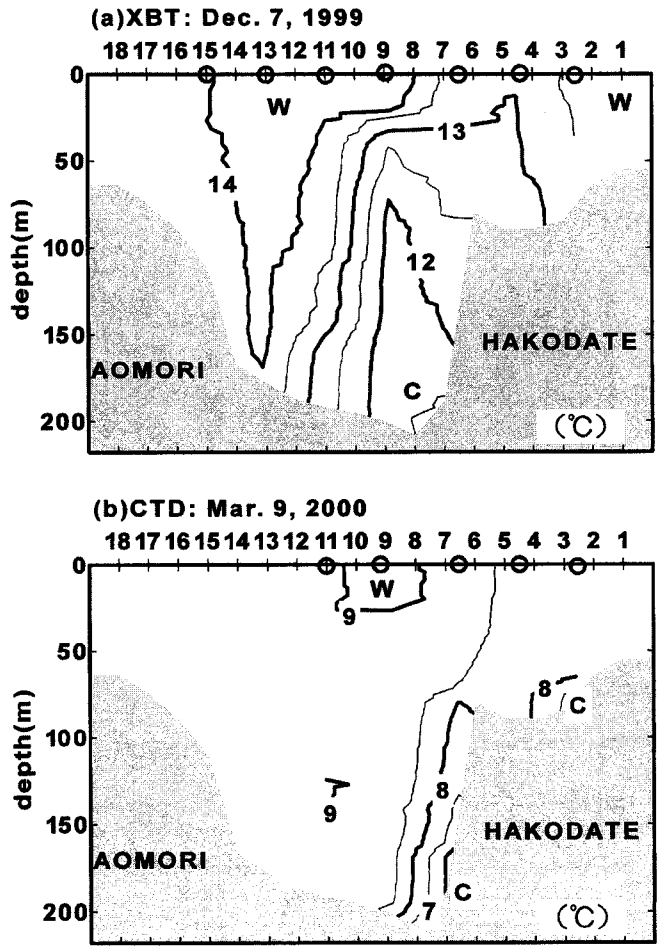

Fig. 4. Across-strait temperature field on December 7, 1999 (a) and on March 9, 2000 (b) calculated from CTD/XBT cast along the observation points shown in Figure 1 (b). Contours give temperature in 0.5°C thin line and 1°C thick line. W: indicate warmer than the surroundings and C: is colder.

of water temperature across the Strait on December 7, 1999 and March 9, 2000, respectively. In December (Figure 4(a)), water of Aomori (southern) side is warmer than that of Hakodate (northern) side, and a weak thermal front is formed around the deeper points (Stns. 9–12). The difference of water temperature across the front is less than 2°C. The entire water column is nearly homogeneous in the vertical, except for the surface water making a weak thermocline (13～14°C). In March (Figure 4 (b)), there is little vertical temperature gradient, and a weak thermal front remains a little near the sea bottom at the deepest point (Stn. 6～7).

Figures 5(a) and (b) show the space-time diagram of NST and the time series of spatial averaged NST across the Strait, measured using the thermistor attached to ADCP instrument. They are temporary averaged using a 3-day running mean filter at each station. Solid lines in Figure 5(a) indicate XBT and CTD observation date and area, respectively. It is interesting that the local maximum temperature of water across the Strait is observed over the deep channels (Stns. 8–15) throughout the study period. This corresponds to the area of warm water observed through XBT/CTD. The spatial averaged NST continuously decreases from 16°C to 8°C for the period of 5 months (Figure 5(b)). If we assume that NST represents the water temperature of vertical mixed water column, the heat loss of ΔQ is estimated by the following equation :

$$\Delta Q = \frac{\rho H C_P \Delta T}{\Delta t}$$

where ρ ($=10^3$ kg • m^{-3}) is the mean water density, C_P ($=4.18$ J • K^{-1} • g^{-1}) the specific heat, H the water depth, and ΔT the temperature difference at Δt time intervals. On substituting $H=150$ m, $\Delta T=-8$°C, and $\Delta t=5$ months, one finds $\Delta Q=-385$ Wm^{-2}. This value roughly coincides with the maximum climatologically winter-time heat loss of 400 Wm^{-2} through the sea surface just west of the Strait, which is estimated by Hirose (1995). These suggest that the vertical mixed water in the Japan/East Sea due to the sea surface cooling in winter enters the Strait, and flows mainly through the deeper part of the Strait during the study period.

Tidal Currents

Current ellipses at K1 and M2 constituents are shown in Figures 6(a) and (b), as the representation of diurnal and semi-diurnal currents. Although the amplitude of O1 current is smaller than that of K1 current by a factor of 0.8–0.9, the phase variations of current ellipses at both the components are almost the same (data not shown). The right-side figure denotes the north. The shaded ellipse indicates the anti-clockwise rotation, and the

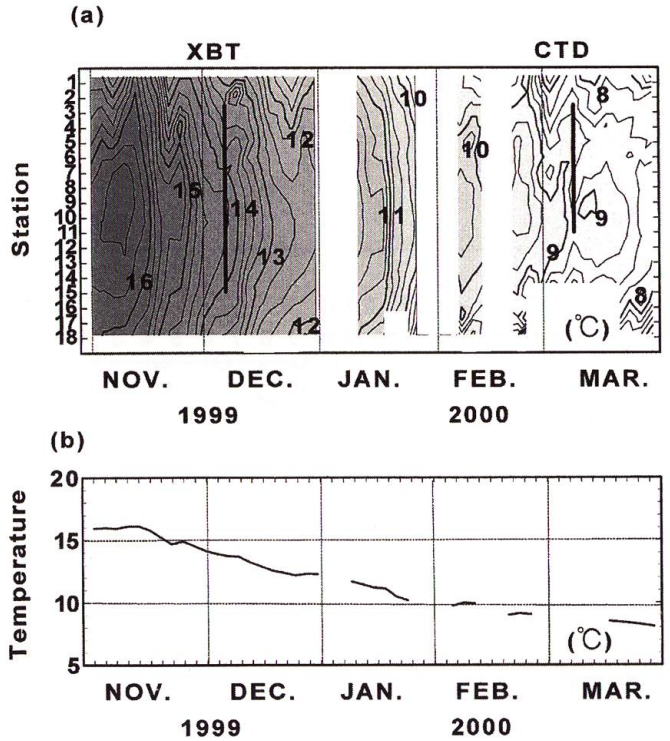

Fig. 5. Space-time diagram of NST measured using a thermistor attached to ADCP (a), and time series of the maximum NST (b). The contour interval is 0.2°C in (a). The solid lines indicate XBT and CTD observation date and area in (a).

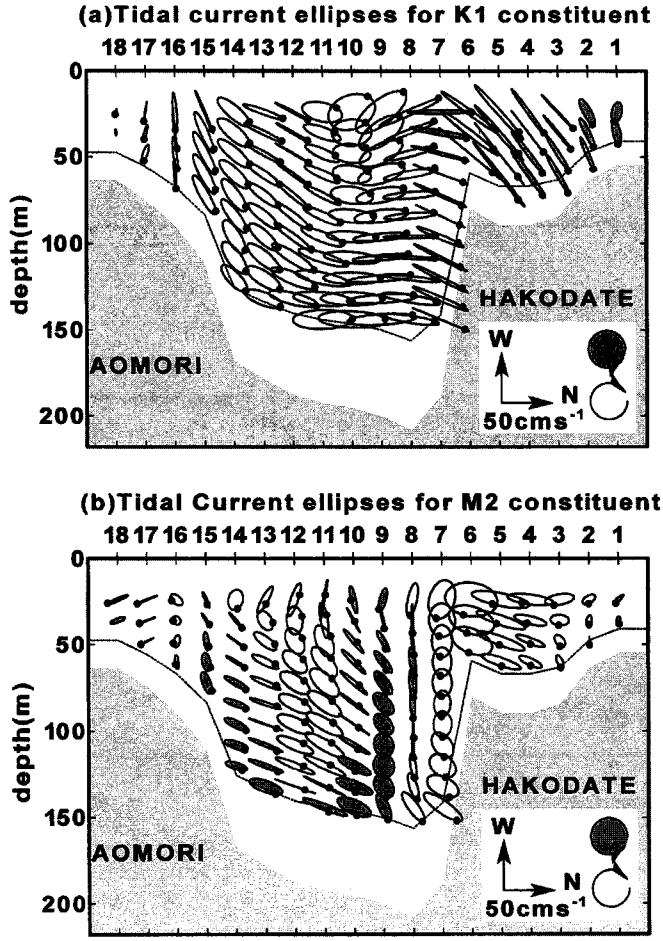

Fig. 6. Tidal ellipses of K1 constituent (a) and M2 constituent (b) in the vertical cross strait section. The shaded ellipse indicates the anticlockwise rotation, and the small solid circle position indicates phase lag.

small solid circle on each ellipses indicates angular measure and reckoned from the lapsed time which the tidal current reached to the maximum value after a tide-generating body passes through the Japanese Standard Longitude (JSL : 135°E).

The amplitudes of K1 current are almost larger than those of M2 current by a factor of 1.0-2.5. The amplitudes of K1 velocity ellipses, therefore, are largest in this section. Although both the ellipses are roughly oriented along the Strait axis (NE-SW direction), their ellipse local inclinations are complicated according to the direction of isobath at each point. Vertical differing phase becomes small in both the constituents, and an entirely barotropic tide would thus appear. The sense of rotation for K1 ellipses around the center of the Strait is clockwise. Its amplitude of K1 tidal velocities at 30-35 cms^{-1} peaks at Stns. 5~6 on the shallow area and their ellipses largely elongate along the local isobath. M2 ellipses are also larger at Stns. 5-6. Note that the sense of rotation for M2 ellipses is more complicated ; i.e., clockwise at Stns. 1-7 and Stns. 11-13, and anti-clockwise at Stns. 8-10 and Stns. 14-15. It is inferred that M2 tide has any transverse oscillation across the Strait.

To investigate the relation between tide and tidal current in the Strait, the tidal volume transports passing through this north-south section are estimated. The harmonic constants of the east-west tidal current component are integrated vertically from bottom to surface. These sinusoidal variations of K1 and M2 volume transports at the origin of phase of maximum tide at Hakodate, are shown in the lower panels of Figures 7(a) and (b). The used tide at Hakodate is well represented as the phase characteristics in the central part of the Strait as shown in Figure 2. The positive transport indicates the tidal current directing to the North Pacific Ocean. The upper panels show the sinusoidal variations of their horizontally total volume transports (Stns. 1-18) and tidal height of K1 and M2 constituent at Hakodate . The phase difference between total volume transport and tidal height is just 90° for M2 tide, and is 129° for K1 tide. The amplitude of M2 tidal height (24 cm) is twice as large as that of K1 tidal height (13 cm), while the total volume transport for K1 (0.72 Sv) is

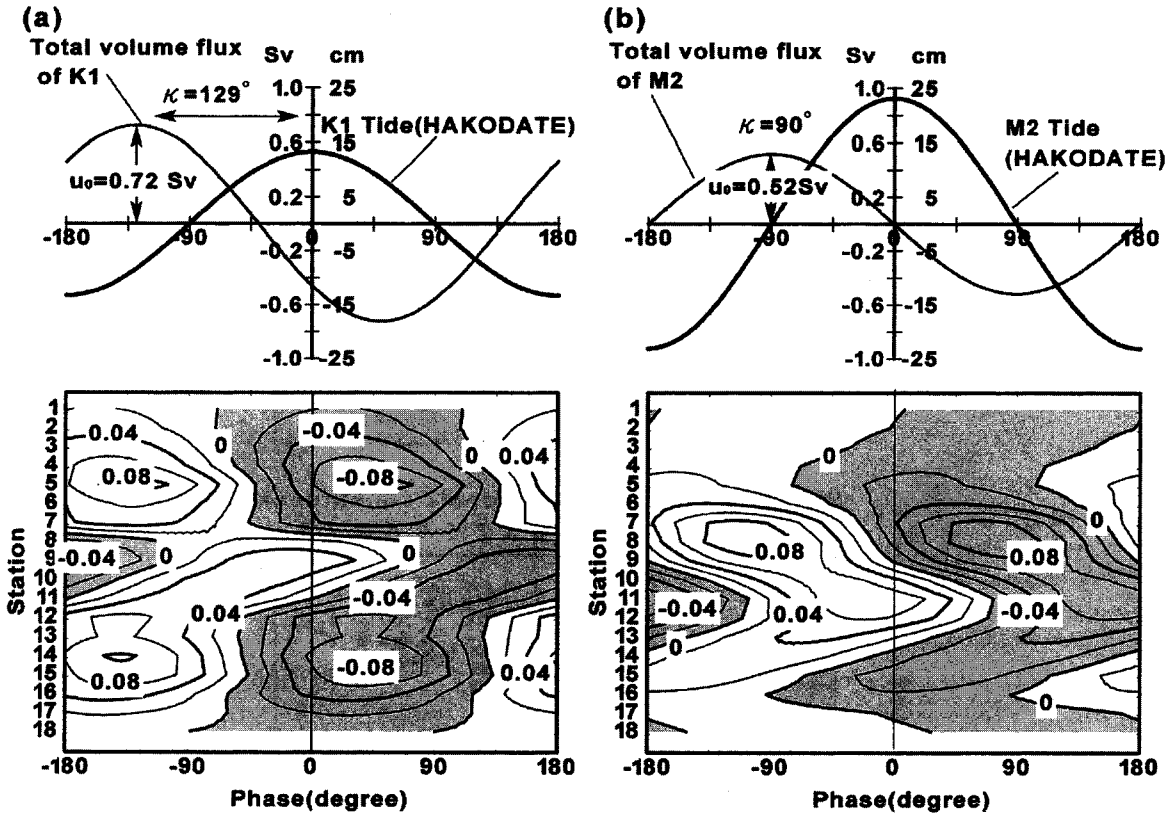

Fig. 7. The relation between the tide of Hakodate and the vertical integrated volume transport of the tidal current in the Strait (K1 (a) and M2 (b)). Sinusoidal variations of the total volume transport of the tidal current to the maximum tide of Hakodate (upper panels), and space-phase diagrams of the vertical volume flux to the phase of the Hakodate tide (lower panels). Contours give transport in 0.02 Sv. The shaded area indicates negative (westward) transport (the tidal current directs to the Japan/East Sea).

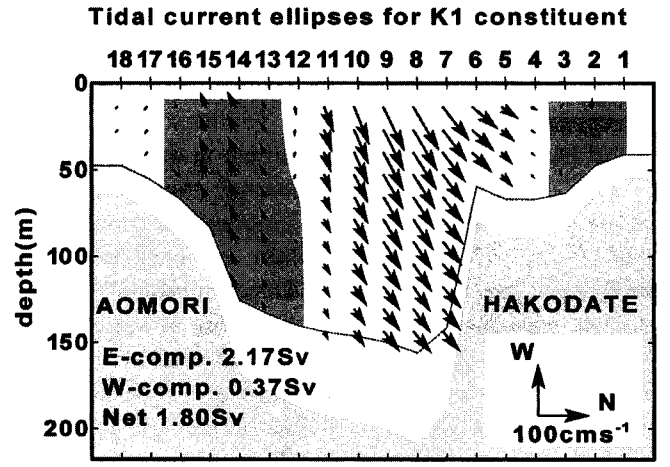

Fig. 8. The mean current vectors during the study period. The shaded area indicates negative (westward) component.

larger than that for M2 (0.52 Sv) by a factor of 1.5. The tidal volume transport at deeper area in the center of observation section lags that at the shallower area by 90°. The main part of volume transport for M2 component is limited to this deep area in the center of the section.

Mean Current during the study period

Four tidal constituents (M2, S2, K1 and O1) are removed from eastward and westward velocity components through our harmonic analysis. This process is conducted for each velocity component at each bin and station independently. After removing the tidal com-

ponents directing to the Japan/East Sea, the mean of all the data obtained during the study period is called a "mean current" in this paper. Figure 8 shows the vertical distribution of mean current vectors. The right-side figure denotes the north, and shaded area shows that the flow has westward component. The maximum current speed of 102 cms^{-1} is observed near the center of the Strait (Stn. 8) and has northeastward flow. The counter (westward) currents appear in the both sides of this northeastward flow. It has been known that the steady clockwise and anti-clockwise circulations exist on the west of Shimokita peninsula and off the coast of Hakodate, respectively (Hori and Nitta, 1978). The northern counter current corresponds with a northern half of an anti-clockwise circulation and same applies to the southern counter current, but the generation mechanism of these circulations are still unknown. Their principal axes face in an almost northeast-southwest direction which consists with the Strait axis, and flow vectors are highly barotropic. Such barotropic flow structure coincides with the nearly homogeneous water column and a weak thermal front as shown in Figures 4(a) and (b).

When the east-west components of mean current are

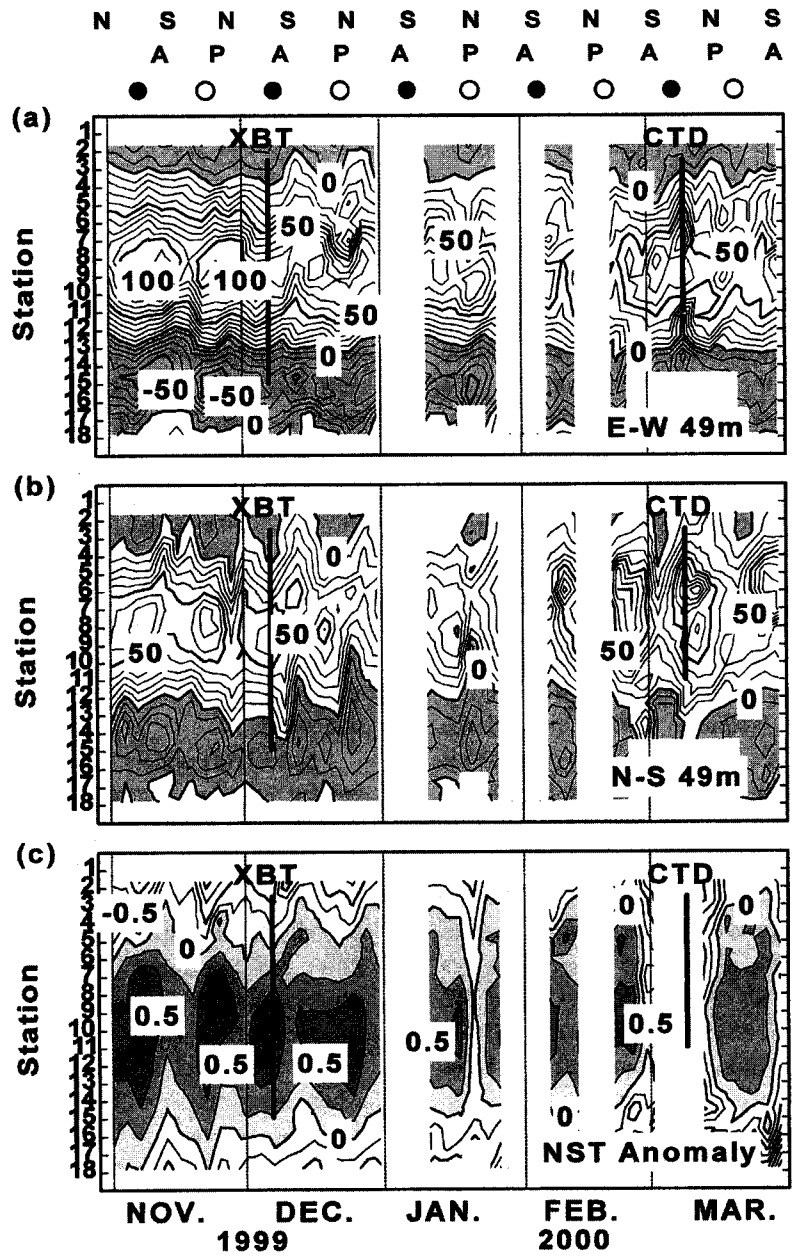

Fig. 9. Time series of the 3-day mean current structure at 48 m E-W component (a), N-S component (b) and 3-day mean NST anomaly (c). The contour interval is 10 cms^{-1} in (a) and (b), and 0.1°C in (c). The solid lines indicate XBT and CTD observation date and area.

integrated vertically from bottom to surface, and horizontally from Stn. 1 to Stn. 18, the volume transports passing through the section are estimated. The eastward and westward volume transports are 2.2 Sv and 0.4 Sv, respectively, so that the net eastward transport of TWC is 1.8 Sv. The past studies have estimated the similar volume transport of TWC. For examples, Shikama (1994) measured the current by utilizing the bottom-mounted ADCP, and estimated annual mean volume transport to be about 1.4 Sv. Onishi and Ohtani (1997) indirectly estimated the inflow transport into the Strait in the period from 1988 to 1993 as the residual transport of the geostrophic flow budget around the western sea area of the Strait and then, its inflow transport was estimated to range from 0.9 to 2.7 Sv.

Subtidal variations

We also investigate the subtidal current variations. We smooth the 3-day data by removing the tidal components and the resultant data are used as sub-samples at 3-day interval. Figures 9(a) and (b) show the space-time diagram of eastward and northward components of velocities at a depth of 49 m. The fluctuations during a fortnightly period are clearly seen between Stn. 5 and Stn. 11 in both the current components. To investigate their periodicity, FFT analysis is performed to the data obtained by averaging the data at Stns. 5 to 11. The lacks of data are complemented with a mean value at each station. The average values per 3 days are obtained from the data in 3 consecutive days in the study period and 51 sets of data in total are obtained. Insufficient number of sets of data were compensated with adding the data as above, and consequently 64 sets of data ($N=2^6$) are obtained. The result is shown in Figure 10. The Nyquist frequency is 0.17 cpd and the degree of freedom is 10. The statistically significant spectrum peak is seen at 13.7 cpd, especially in the north-south current component.

We must need to check the possibility that fortnightly variation may be an apparent phenomenon due to the remains of active tidal constituents, i.e., aliasing period. When the sampling interval is 0.25-0.5 days (2-4 times per day), the aliasing periods estimated from O1 and M2 constituents are 14.2 and 14.8 days, respectively. However, the fortnightly amplitude velocity inferred from Figure 9(b) which ranging 10~30 cms^{-1} is much larger. If there remain active tidal constituents, the residual tidal variability will be much smaller than this velocity. In fact, Shikama (1994) preformed ADCP observation at the sampling intervals of 10 to 20 minutes, and reported that the significant fortnightly variation with amplitude of about 0.6 Sv existed in the Strait. Hikosaka (1953) has already found the current variations with the periods

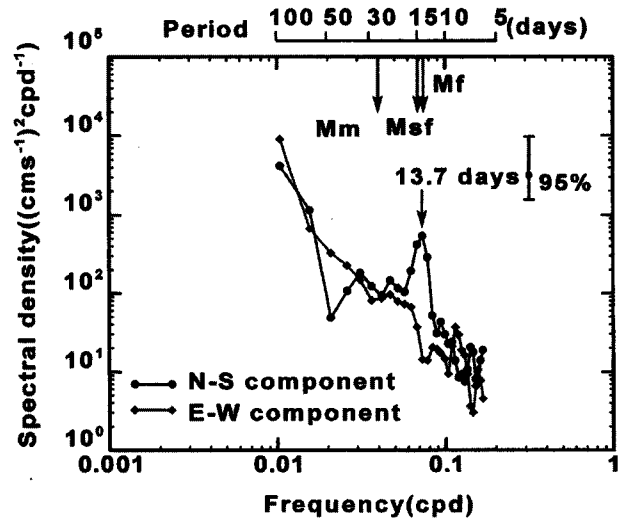

Fig. 10. Power spectral densities of the eastward (diamond) and northward (solid circle) component average flow velocity data at Stns. 5-11 in 48 m depth.

of about a fortnight or a month in the 40-days observation by Ekman-Mertz current meter at the west entrance of the Strait. Furthermore, we can also find the similar variability as above in the time series of NST. Figure 9(c) shows the space-time diagram of the 3-day mean NST anomaly, which is the deviation from the time series of spatial averaged NST across the Strait (Figure 5(b)). That is, figure represents the spatial variation of NST structure across the Strait after removing the seasonal cooling effect. In comparison with current variations, the area between Stn. 8 and Stn. 14 tends to be relatively warmer when the eastward or northward current components increase, i.e., a fortnightly large inflow of warm water from the Japan/East Sea is suggested.

Figure 11(a) shows the time series of the north-south current velocity obtained by averaging the data at Stns. 5 to 11. Using this time series, we select the time when the local velocity becomes maximum (solid diamond) and minimum (open diamond). To investigate the overall current structure difference between the maximum and minimum values, the mean current vectors observed when the current becomes maximum are subtracted from those when the current becomes minimum. Figure 12 shows the current vector differences, where the parts of halftone meshing are the area that the difference is not significant ($p>0.05$) according to Student's t-test. The significant difference appears around the center, and the variation of a barotropical northeast flow can be roughly suggested. Considering the difference of east-west current components, the transport amplitude of fortnightly variation, which is obtained by multiplying the average of east-west current components

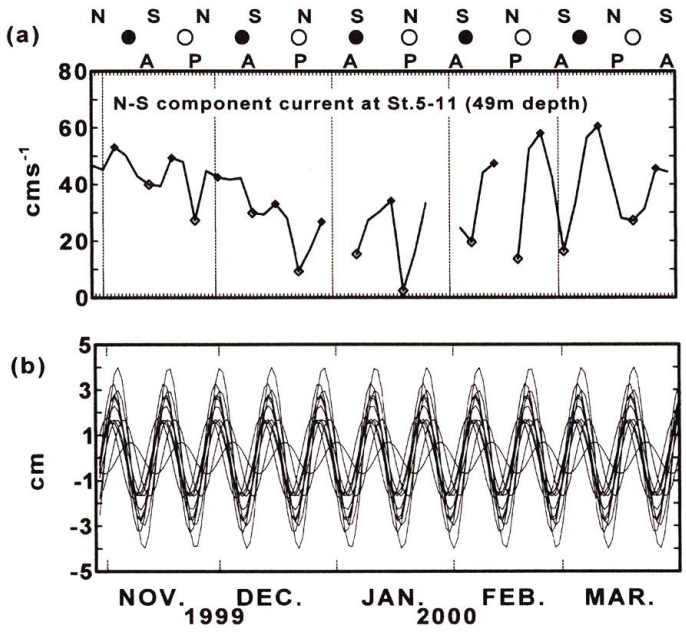

Fig. 11. Time series of the averaged mean northward component current velocity at Stns. 5–11. Solid circles indicate the local maximum velocity and open circles the local minimum velocity (a). The sinusoidal variations of Mf tide at the 12 typical tide points of the Japan/East Sea, near the west entrance of the Strait (b). The location of the tide points is shown in Figures 14(a) and (b), and equivalent to the solid circle area shown in uppermost figure of Figures 14.

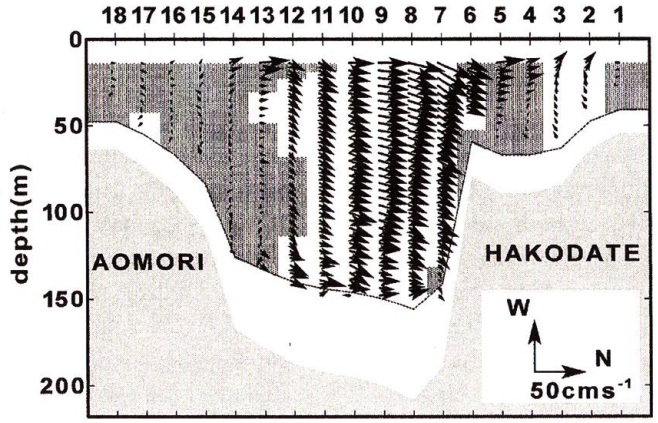

Fig. 12. Difference of the maximum time point deduce the minimum time point in Figures 11(a). The parts of meshing are the area that the difference is not significant ($p>0.05$) according to Student's t-test.

between Stns. 7 and 11 (9 cm) by the cross section of this area (18.5 km×200 m), is about 0.3 Sv.

The estimation of the flow using this method is performed since ADCP data acquisition rate is low in February and March, especially in lower layers, and snapshot factors can be included even in the average value. In addition, this estimation method is thought to be appropriate since the general structure of fluctuations tend to be barotropic and is not vertically noticeable. Although the remarkable countercurrent is observed in the Hakodate offing, the flow in this area is small (−0.05 Sv).

Discussion

Dynamics of tides in the Strait

Our long-term current observation in winter using the ship-mounted ADCP shows that major tidal constituents are almost barotropic, but their directions of major axes and amplitudes are largely distorted by local geographical features. Therefore, we will discuss the tidal volume transport of each constituent across the Strait which is integrated across the transect. First, the volume transport amplitudes and phases for M2, S2, K1 and O1 constituents obtained through our study are compared with those proposed by Odamaki (1993) in Table 2. Odamaki (1993) calculated the volume trans-

Table 2. Comparisons with phases and transport between present study and Odamaki (1993)

	Present Study		Odamaki (1993)	
	Q (Sv)	κ (°)	Q (Sv)	κ (°)
M2	0.52	205	0.83	167
S2	0.24	243	0.28	226
K1	0.72	228	1.34	206
O1	0.60	215	1.04	196

ports near the western entrance of the Strait, which located about 30 km west from our transect. His data were based on the short-term mooring observations only at 2 points. Amplitudes and phases from two studies showed similar trends. Our amplitudes are 50-60% less than his data for M2, K1, and O1 ; and about 80% less for S2. A maximum difference by a factor of 2 is observed for K1 constituent. Phase differences between the two studies range from 20° to 40° for all the constituents, and our phases are always larger than his. This may be caused by the differences in the observed locations. Relatively larger amplitude of Odamaki (1993) may be obtained due to the overestimation caused by the limitation in the vertical resolution.

Ogura (1932) recognized that the tides in the Strait occurred as the superimpose of incidental waves into the channel from the connecting two basins which were independent on each other in tidal motion. The phase charts in Figures 2 indicate that, at both sides of the Strait, M2 and K1 tides are in-phase and nearly out of phase, respectively, and the tide amplitude of constituents is higher in the North Pacific Ocean than that in the Japan/East Sea. In K1 tide (Figure 2(a)) ; the amplitudes along the northern coast are remarkably larger by a factor of 2 than those along the southern coast. The phase of K1 tide rapidly changes from 180° to 360° near the western entrance. However, the amphidromic point, which usually appears based on the earth's rotation, is not formed. The phase difference between our estimated tidal current transport and the tide at Hakodate for M2 constituent is just 90° as shown in Figure 7(b). This implies that M2 tide occurs as a standing wave, which has been already recognized by Ogura (1932).

However, the phase difference for K1 constituent is about 129°. Considering that K1 tide is composed of the standing and progressive waves, K1 tide could be decomposed into these two waves by using the above mentioned phase difference. In Figure 7(a), we assume that K1 tide variation at Hakodate is represented by a cosine-function with a frequency of ω, and current amplitude and phase difference between tide and current are u_0 and κ, respectively. Then, the tidal current variation with a cosine function can be easily decomposed by the following two functions :

$$u_0 \cos(\omega t - \kappa) = u_p \cos \omega t + u_s \sin \omega t.$$

The cosine and sine functions on the right indicate the progressive and standing waves, respectively. When the transport amplitudes of progressive and standing waves are u_p and u_s, respectively, the relations between these parameters are as follows :

$$u_0^2 = u_p^2 + u_s^2$$
$$\tan \kappa = u_s / u_p$$

Using these formulas and observed values of $u_0 = 0.72$ Sv and $\kappa = -129°$, we get $u_p = -0.45$ Sv and $u_s = -0.56$ Sv. Based on this result, it is inferred the magnitudes of standing and progressive waves are almost the same ($| u_p | \approx | u_s |$), and the propagating direction of progressive wave is westward from the North Pacific Ocean to the Japan/East Sea, because u_p is negative. If we consider the existence of incidental Kelvin wave from the Pacific Ocean for K1 tide, relatively high tide along the northern coast and disappearance of the amphidromic point near the western entrance can be understood.

The fortnightly current variations

In this subsection, we will discuss the possible causes of fortnightly current variations. The first possible cause is the density driven current which occurs due to a spring-neap periodic change based on the modulation of the vertical mixing intensity associated with the variations of tidal current; e.g., "Kyucho" observed in the Bungo channel, Japan, by Takeoka et al. (1993). However, the water observed during the study period is vertically well mixed due to the sea surface cooling. Therefore, the modulation of the vertical mixing intensity associated with the variation of tidal currents is not a main cause for this fortnightly variation. The second possible cause is the periodical sea surface wind forcing. To investigate the phase relation, we perform the cross-correlation analysis between the 3-day mean value of northward current of ADCP and that of both the north-south and east-west components of wind at Hakodate (Figures 13(a) and (b)). A broad peak is seen around the 14 cpd of the experiment in east-west wind component, but the coherences are not statistically significant.

The third possible cause is the long-period lunar tides with a fortnightly period ; i.e., Mf (13.7-day period) and Msf (14.2-day period) tides. It has generally been accepted that the long-period tides are well approximated by their equilibrium forms, especially around the Japanese islands. Their tidal amplitudes may be

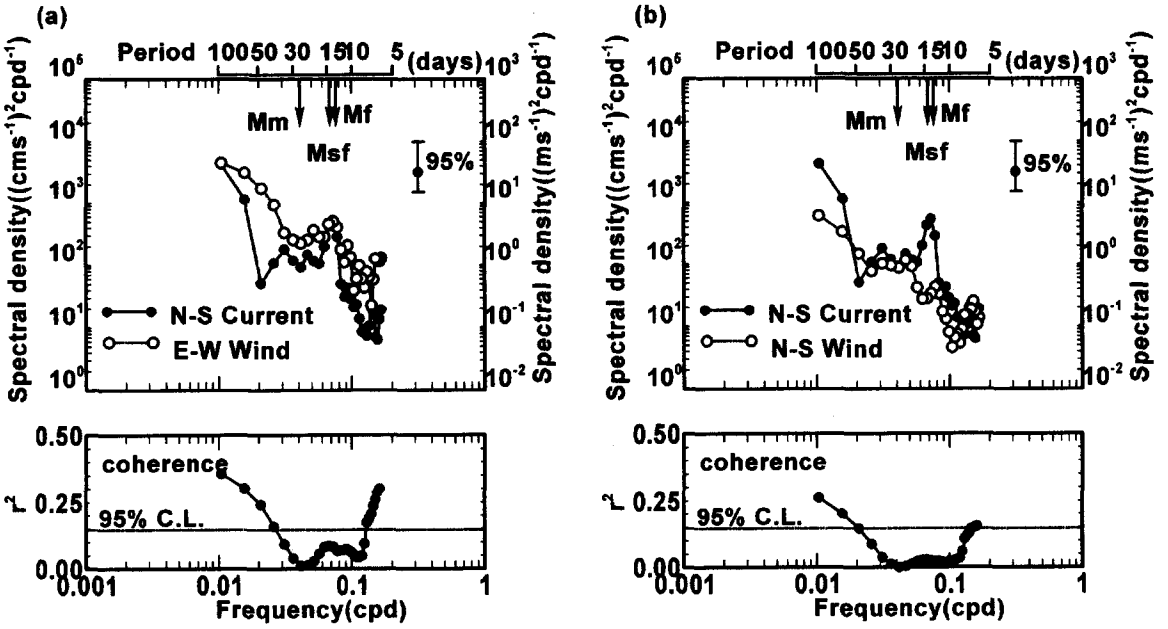

Fig. 13. Cross-spectral-coherence between the 3-day mean value of north-south component of mean current and that of long-strait (east-west component) wind data, power spectral densities (upper), and coherence-squared (bottom) (a). Coherence between the 3-day mean value of north-south component of mean current and that of cross-strait (north-south component) wind data (b).

sufficiently small because the nodal line of the long-period tidal potential is just running at the central part of the Japan islands (35.26° N). However, we present a different view of the non-equilibrium response to the fortnightly tidal forcing in the Japan/East Sea. Tidal harmonic constants for Mf and Msf tides in the region around the Strait investigated by the Japan Marine Safety Agency (1992) are shown in Figures 14(a) and (b), respectively. The amplitude of tide is represented by a radius of circle and plotted at each location (left panels). The unit of phase degree is used for the phase lag referring to the local transit of JSL. When the amplitude of tide is less than 0.5 cm, the corresponding phase is not plotted because the background noise is expected to be large. The phase versus latitude is shown in the right panels by using the different marks at each sea area (the phase faced on the Japan/East Sea: ●, the Pacific Ocean: ○ and the Tsugaru Strait: ◐).

It is found that the amplitude for Msf tide is small and the phases are largely scattered, compared to those for Mf tide. The Mf tide is more energetic along the coast faced on the Japan/East Sea and the Strait with the amplitude of 1-3 cm. Their phases (● ◐) are roughly uniform around 200° within the limits of about 60°. Such distributions suggest the well-organized spatial structure of Mf tide in the Japan/East Sea, but the reason for this is beyond the scope in the present study. In contrast, the amplitudes for Mf tide in the North Pacific Ocean are much smaller (less than 1cm), and the difference of amplitude between both sides of the Strait is expressed by a factor of approximately 3-4. We can expect the oscillation flows in the Strait are generated by the sea level difference between both sides of the Strait.

A simple and revealing approach to the study of low frequency flow through straits has been developed by Wright (1987). He considered the periodical exchange through a strait (W, L and H are the width, length and depth) separating two semi-infinite basins under the assumption of inviscid along-strait momentum balance. According to Wright (1983), the amplitude Q of oscillated volume transport caused by sea level difference through straits and θ of phase difference between the sea level difference and the volume transport is expressed as follows:

$$Q=\sqrt{\frac{(gH(W/\omega L)\cdot(\overline{\zeta_1}-\overline{\zeta_2})^2)}{1+(fW/\omega L)^2}}$$

$$\theta=\tan^{-1}\left(-\frac{1}{fW/\omega L}\right)$$

where ω is the radian frequency; g is the acceleration due to gravity; f is the Coriolis parameter; $\overline{\zeta_j}$, ($j=1$, 2) and is the spatially averaged sea level amplitude over the basins. The dimensions of the Strait are $L=100$ km, $W=30$ km, and $H=150$ m. The radian frequency of Mf tide is; $\omega=0.53\times10^{-5}s^{-1}$; and $f=9.66\times10^{-5}$ s^{-1} (41.5°CN), $\zeta_1=1\sim3$ cm in the Japan/East Sea coast, and $\zeta_2\approx0$ cm in the adjacent coastal area of the Strait facing the North Pacific Ocean. The amplitude of the tidal transport of Mf constituent through the Strait is

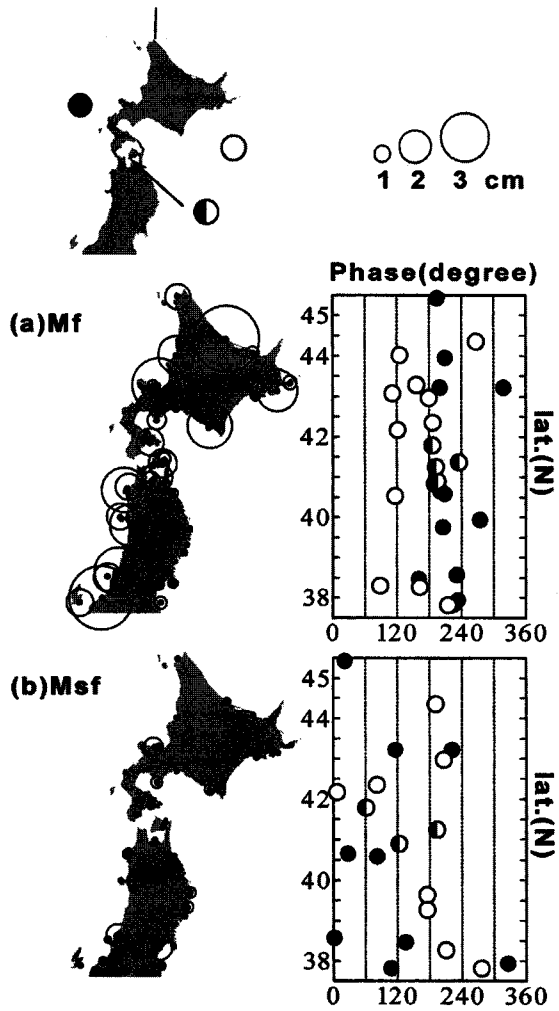

Fig. 14. Amplitude (left) and phase (right) distributions of the tide around the Tsugaru Strait for Mf constituent (a) and Msf constituent (b). The marks indicate each sea area (faced on the Japan/East Sea ●, the Pacific Ocean ○ and the Tsugaru Strait ◐). The unit of phase degree is used for the phase lag referring to the local transit of JSL (135° E). The amplitude of tide less than 0.5 cm and the corresponding phase is not plotted.

Q=0.15~0.45 Sv, and phase lead to 10° (tide lead tidal current). Figure 11(b) shows sinusoidal variations of Mf tide at the 12 tide point of the Japan/East Sea and the Strait. The phases in these Figures showing fortnightly fluctuations are in very good agreement with each other. As described in Section 4.4, the difference in the passage volume flux between maximum and minimum, which is thought to be caused by the fortnightly fluctuations calculated based on the mean of the 3-day currents (the mean current) excluding the tidal components, is 0.3 Sv. This is within the range of the above theoretical value. Although the actual strait has complicated geophysical features, the theoretical values are calculated based on the assumption that the geometry of the Strait is simple. However, it can be said that the theoretical values are in good agreement with the observation values. Why the fluctuation appears not on the strait axis (in an east-west direction) but in a north-south direction may be explained by the relation between the direction of the major axis of tidal current ellipses and that of the mean flow. With the assumption that the center of the Strait is broad crank-shaped canal, the mean current, which is the quasi-steady current, flows in one direction from the Japan/East to the North Pacific Ocean. The current flow is strong in the strait axis in an east-west direction. As described in Section 4.3, the both ends of this axis that is influenced by the local geophysical features have the detached vortical currents, and the counter current, which is thought to be a part of the above currents, is observed (Figure 8). On the other hand, the tidal current is the reciprocating current that does not become steady. The flow direction of the tidal current that trends from the Japan/East Sea to the North Pacific is rapidly shifted northward due to presence of the Shimokita Peninsula in the southern side of an observation cross section, while the direction of the current trending from the North Pacific Ocean to the Japan/East Sea is shifted southward due to presence of the Oshima Peninsula in northern side of the section. When expressing these current conditions as an ellipse of tidal currents, the long axis is thought to be in a north-south direction. The remarkable fortnightly fluctuation is also observed in a north-south direction. These results suggest the possibility that the driving forces inducing the fortnightly fluctuation are not one-way motions such as strength and weakness of a prevailing wind, but reciprocating motions. Therefore, we dare to make reference that Mf constituent is one of the most possible causes of the fortnightly fluctuation.

Conclusions

ADCP monitoring observation is performed at the central basin of the Tsugaru Strait from October 1999 until March 2000. Sea surface cooling is active, and the entire water column is nearly homogeneous. The diurnal tidal current is larger than semi-diurnal tidal current in the center of the Strait. K1 constituent is the most dominant tidal current in this transection. The current of M2 constituent is revealed to have the structure in a lateral direction. The reason for this should be clarified through a model calculation in the further studies.

As with the relation between tidal current transport and the tide at Hakodate, the diurnal constituents are progressive wave-like while the semi-diurnal constituents are standing wave-like. These results are not

contradictory to the phase differences of the tidal current in the Strait suggested by other researches. However, the amplitude of the tidal current differs greatly.

Our estimation of the mean current is 1.8 Sv eastward (details: the eastward volume transport is 2.2 Sv and the westward transport is 0.4 Sv). Since the flow vector has small vertical variations in its length and direction, it can be said to have barotropic tendency. This value is similar to the values described in the previous studies, which have been obtained in the short term and through indirect measurements or have included snapshot factors. ADCP monitoring observation using a regular ferry has been maintained at present, and the changes of the volume transport in each season including stratification period will be investigated in future.

The significant fortnightly fluctuation is observed in the mean current. The averaged value of the difference in the passage volume transport between maximum and minimum is 0.3 Sv. This fluctuation has no statistically significant correlation with wind forcing. The prevailing direction of fortnightly fluctuations indicates the current is reciprocal, and the phases of Mf constituents at 12 tide points near the Strait in the Japan/East Sea are almost same as those of these fluctuations. In addition, the phases of these fluctuations are in good agreement with theoretical values (0.15-0.45 Sv) estimated based on the sea level difference between amplitude of Mf constituents in the Japan/East Sea and that in the North Pacific Ocean. It is thought that Mf constituent is the most possible cause of the fortnightly fluctuation. The reasons why the amplitude of Mf constituents in the Sea of Japan is large can not be explained by the potential tidal power, and have not been clarified yet. The further study will be conducted in larger areas to investigate the reasons.

Acknowledgements

We express our gratitude to the HIGASHINIHON-FERRY Co., Ltd. and the crew of M.V. *VIRGO* for the cooperation to our monitoring. We are also grateful to Captain Sugisawa and crew of R.V. *MIZUHO* for the assistance with the XBT and CTD field work. The present study is partially supported by Grants—in Aid for Scientific Research (project No. 12480145) and the NEAR-GOOS (North East Asian Regional-Global Ocean Observing System) Project, from the Ministry of Education, Science and Culture, Japan. Michihiro Shonai gave useful advice about the analysis technique and program languages.

References

Hikosaka, S. (1953) On the ocean-currents (Non-tidal Currents) in Tsugaru Strait. *Hydrographic bulletin*, **39**, 279-285 (in Japanese).

Hirose, N. (1995) Heat Budget in the Neighboring Seas around Japan. 1994-1995 *Master's Thesis, Kyushu University*, Fukuoka, Japan, unpublished.

Hori, S. and K. Nitta (1978) The elucidation of the seawater flow mechanism in Tsugaru Strait. *Science and Technology Agency Research Coordination Bureau, Research report*, 14-53 (in Japanese).

Ishikawa, K., S. Shibata, and T. Miyao (1986) Sea structure of Tsugaru Strait. *Marine Science Monthly,* **19**(1), 1987, 34-39 (in Japanese).

Japan Marine Safety Agency (1992) TIDAL HARMONIC CONSTANTS TABLES JAPANESE COAST, *Japan Hydrographic Association*, Tokyo, 267 p.

Kubota, T. and K. Iwasa (1961) On the Current in Tugaru Strait. *Hydrographic bulletin*, **65**, 9-26 (in Japanese).

Nitani, E., K. Iwasa, and W. Inada (1959) On the Oceanic and Tidal Current Observation in the Channel by making Use of Induced Electric Potential. *Hydrographic bulletin*, **61**, 14-23 (in Japanese).

Odamaki, M. (1984) Tide and tidal current in Tsugaru Strait. *Bulletin on Coastal Oceanography*, **22**, 12-22 (in Japanese).

Odamaki, M. (1989) Co-Oscillating and Independent Tides of Japan/East Sea. *Journal of the Oceanographycal Society of Japan*, **45**, 217-232.

Odamaki, M. (1993) Relation of Tidal Response and Tidal Currents. *Report of Hydrographic Researches*, **29**, 87-98 (in Japanese).

Ogura, S. (1932) The tide of Tsugaru Strait. *Hydrographic bulletin*, **110**, 1-26.(in Japanese)

Ogura, S. (1933) The tides in the seas adjacent to Japan. *Report of hydrographic researches*, **7**, 1-189.

Ogura, S. (1934) Tide. Iwanami complete book. 252 p. (in Japanese)

Shuto, K. (1982) A review of sea conditions in the Japan/East Sea (I). *Umi to Sora*, **57**, 157-169. (in Japanese)

Shikama, N. (1994) Current measurements in the Tsugaru Strait using bottom-mounted ADCPs. *KAIYO MONTHLY*, **26**, No. 12, 815-818 (in Japanese).

Takeoka, H., H. Akiyama, and T. Kikuchi (1993) The Kyucho in the Bungo Channel, Japan—Periodic Intrusion of Oceanic Warm Water. *Journal of Oceanography*, **49**, 369-382.

Wright, D.G. (1987) Comments on "Geostrophic Control of Fluctuating Barotropic Flow through Straits". *Journal of Physical Oceanography*, **17**, 2375-2377.